INTERNATIONAL JOURNAL OF CLIMATOLOGY, VOL. 16, 1281–1296 (1996)

THE INFLUENCE OF CLOUDS ON THE RADIATION BUDGET OF ICE AND SNOW SURFACES IN ANTARTICA AND GREENLAND IN SUMMER

RICHARD BINTANJA AND MICHIEL R. VAN DEN BROEKE
Institute for Marine and Atmospheric Research Utrecht, Utrecht University, Princetonplein 5, 3584 CC Utrecht, The Netherlands
email: bintanja@knmi.nl

Received 23 August 1995
Accepted 15 January 1996

ABSTRACT

Shortwave and longwave radiative surface fluxes over four different types of highly reflective surfaces are presented, with the emphasis on the dependence of these fluxes on total cloud coverage. Measurements were performed in summer during three field campaigns: one in Greenland and two in Antarctica. It was found that especially the strength of the dependence of the shortwave fluxes on cloud amount differed widely among the four locations; this is due to differences in surface albedo and cloud shortwave transmissivity. At two locations the net allwave radiation was found to increase with increasing cloud coverage (sometimes referred to as the 'radiation paradox'). It is demonstrated that this is due mainly to the fact that the shortwave cloud transmissivity at these sites is relatively high, which, in turn, is thought to be caused mainly by a low cloud optical thickness and by multiple scattering between surface and cloud-base. Whether or not the net surface radiation increases with increasing cloud coverage is found to depend chiefly on the values of the surface albedo and effective shortwave cloud transmissivity.

KEY WORDS: Antarctica; Greenland; radiation; clouds; snow and ice

INTRODUCTION

The radiative fluxes are important elements of the Earth's climate system. In particular the impact of clouds on the radiative fluxes is a matter of great interest for climate sensitivity studies, for example, but is also one of great uncertainties (Crane and Barry, 1984; Arking 1991). For instance, satellite radiation studies have shown that clouds tend to warm the earth–atmosphere system over the highly reflective polar regions, in contrast to their effects in other regions (e.g. Stephens *et al.*, 1981; Nakamura and Oort, 1988). Recent studies, however, indicate that also over the polar regions clouds have a net cooling effect (Li and Leighton, 1991; Schweiger and Key, 1994). Probably, this can be attributed to the fact that recent studies revealed that clouds have a cooling effect in the shortwave part of the spectrum (Nemesure *et al.*, 1994), in contrast to the warming effect found in the earlier studies. Even less is known about the influence of clouds on the surface radiation budget over snow and ice in the polar regions. This is largely caused by the fact that knowledge has to be gained from local surface observations, which are scarce owing to high expedition costs.

The shortwave and longwave radiative fluxes are an important part of the surface energy balance over snow and ice surfaces. In particular, radiation provides a significant part of the energy used for melt in ablation areas of glaciers and ice caps, in spite of the relatively high albedo of such surfaces (e.g. Greuell and Konzelmann, 1994; Bintanja, 1995). Changes in the radiative fluxes in those regions caused by climatic variations can thus have significant consequences for (short-term) fluctuations in global sea level. Also, because cloud amount and properties may change under varying climatic conditions, it seems worthwhile to investigate what influence clouds have on the radiative fluxes over snow and ice.

Some local observational studies in polar regions in summer have demonstrated that over highly reflective snow fields the net surface radiation budget increases with cloud amount (e.g. Holmgren, 1971; Jacobs *et al.*, 1972;

CCC 0899-8418/96/111281-16

Ambach, 1974; Ohmura, 1981; Yamanouchi *et al.*, 1982; Wendler, 1986). This is in contrast to what happens more generally over low reflective surfaces. Some model-based approaches have been undertaken that have yielded insight in this phenomenon (e.g. Schneider, 1972; Stephens and Webster, 1981; Tsay *et al.*, 1989; Curry and Ebert, 1992; Schweiger and Key, 1994). Stephens and Webster (1981) use a Radiative–Convective Model (RCM) to investigate the effect of cloud properties on the surface radiation budget. They concluded that clouds tend to warm the surface (due to the fact that enhanced longwave input is larger than shortwave reflection) when either (i) the clouds have a small liquid water content and hence low albedo, (ii) the clouds are located at higher levels in the atmosphere, (iii) the clouds are located close to the pole where insolation is low, or (iv) the surface albedo is high. Their model results for a winter situation suggest that all clouds in the polar regions (irrespective of surface albedo) and high clouds in the (sub) tropical regions tend to warm the surface. The latter result confirmed the findings of the RCM study of Manabe and Wetherald (1967).

The increase of net surface radiation with increasing cloud amount is sometimes called the 'radiation paradox' (Ambach, 1974), and is due to the fact that with increasing cloud amount, the increase in net longwave radiation dominates over the decrease in net shortwave radiation. Because it is not really a paradox, we will abandon the term 'radiation paradox' here.

In this paper, we will show how the surface radiation budget depends on cloud coverage, and how this dependency is influenced by the surface albedo and the shortwave cloud properties. We will use radiation data collected over four different types of highly reflective surfaces. Results from some of the above-mentioned model studies will be used to explain qualitatively the features that are observed. This study provides insight in the important mechanisms that determine the radiative fluxes over highly reflective surfaces from an observational point of view.

INSTRUMENTATION AND METHODS

In our analysis we will use radiation data over four different highly reflective surface types. The four locations differ mainly with regard to surface albedo, cloud amount, predominant cloud optical thickness and surface temperature. The shortwave radiation budget was measured directly at all four locations, the surface of the ice/snow being always practically horizontal. Problems with the longwave radiation measurements at some of the locations forced us to estimate the longwave radiation budget using either radiative transfer models, empirical relationships or surface energy balance models. However, it will be shown that spatial variations in the dependence of net longwave radiation on cloud amount are much less important than those concerning net shortwave radiation. The four locations, which are indicated in Figure 1, will be described below.

(I) The ablation zone in the western part of the Greenland ice sheet (67°N, 50°W). The surface of this location consisted of melting ice at an elevation of 340 m a.s.l., 2·6 km from the ice edge. The broadband shortwave radiation budget (Kipp CM14) was measured continuously from 9 June to 31 July 1991 during the Greenland Ice Margin Experiment (GIMEX) (Oerlemans and Vugts, 1993). The surface temperature was 0°C throughout the entire period. Incoming longwave radiative fluxes ($L\downarrow$) were measured directly but were judged to be very inaccurate. Therefore, incoming longwave radiation was estimated from the empirical relationship of Konzelmann *et al.* (1994), which was derived from daily averaged longwave radiation measurements near the equilibrium line on the EGIG transect (approximately 300 km north of location I):

$$L\downarrow = \left\{(0{\cdot}23 + 0{\cdot}483(e_a/\theta_a)^{1/8})(1 - N^3) + 0{\cdot}963N^3\right\}\sigma\theta_a^4 \tag{1}$$

in which e_a (Pa) is the water vapour pressure at screen level, θ_a (K) is the screen-level temperature, N (1/10) is the total cloud amount and σ ($= 5{\cdot}667 \times 10^{-8}$ W m^{-2} K^{-4}) is Stefan–Boltzmann's constant. The quantities e_a and θ_a have been measured at approximately 2 m above the ice surface.

(II) The ablation area of the Ecology Glacier, which is an outlet glacier of the King George Island ice cap (62°S, 58°W, 100 m a.s.l.). King George Island is situated at the northern tip of the Antarctic Peninsula and experiences a relatively warm, maritime climate (the annual mean temperature is −2°C). During the experiment (17 December 1991 to 16 January 1992), the surface consisted mainly of melting snow. The shortwave radiative fluxes were measured continuously with Aanderaa 2811 sensors. Incoming longwave

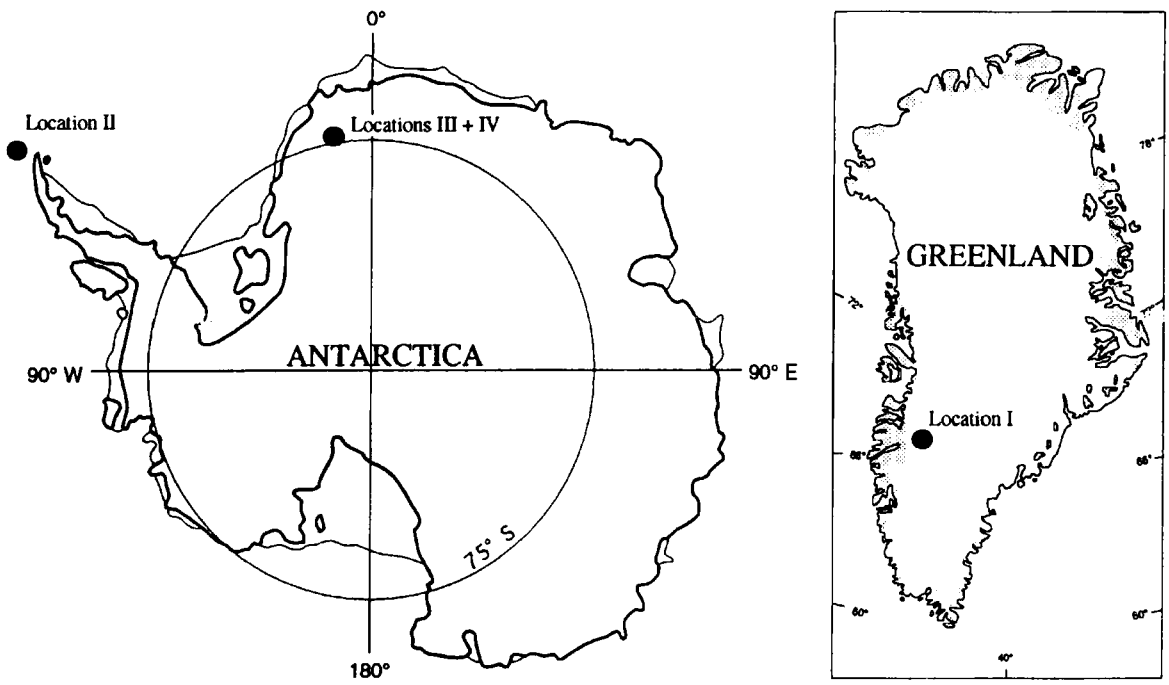

Figure 1. Geographical setting of the four locations used in this study.

radiation was not measured. Instead, L↓ was calculated with a broad-band emissivity radiative transfer model, because simple empirical relationships such as equation (1) are likely to be valid only for the same (type of) location where they are derived and are therefore not uniformly applicable. This radiative transfer model uses as its most important input: vertical temperature and moisture profiles as obtained from balloon soundings in the lowest kilometre, the subarctic summer temperature, humidity and ozone profiles from McClatchey *et al.* (1971) above 1 km, and observed cloud amount and cloud-base height (this was estimated either visually with the aid of the local topography or using vertical profiles of humidity). CO_2 is assumed to be uniformly mixed, with a volume mixing ratio of 350 ppmv. The emitted longwave radiation was estimated using a surface energy balance model that computes ablation, vertical snow/ice temperature distribution, surface heat fluxes from measured meteorological quantities and radiative fluxes (Bintanja, 1992, 1995). Snow and ice surfaces are generally considered to be virtually black for infrared radiation (Brutsaert, 1982), and we will therefore assume that the surface emissivity of snow and ice equals unity. The surface temperature was found to be 0°C for 80 per cent of the time.

(III) The dry snow surface of the Antarctic plateau in Dronning Maud Land (74°S, 11°W, 1200 m a.s.l.). The shortwave radiation budget (Kipp CM14) and the incoming net radiation (Aanderaa 2770) were measured continuously from 1 January to 10 February 1993. The outgoing longwave radiation was evaluated using a surface energy balance model (Bintanja and Van den Broeke, 1994, 1995). This model calculates the surface energy fluxes and the (sub) surface temperature distribution with measured meteorological quantities as input. The surface temperature was found to remain below −5°C during the entire measuring period.

(IV) An Antarctic blue ice area in Dronning Maud Land (74°S, 11°W, 1150 m a.s.l.). The distance to location III is approximately 5 km. Instruments and methods similar to location III were used to obtain the radiative fluxes from 4 January to 10 February 1993. The surface temperature remained below 0°C throughout the measuring period.

Various test campaigns and calibration sessions were undertaken, often before and after each expedition, to determine the precision of the sensors. These, and also intercomparison of sensors during some of the field campaigns, have shown that the sensor precision of the Kipp CM14 and the Aanderaa 2811 is 2 per cent and that of

Table I. Characteristics of the four measuring locations. Surface air temperature (θ_a), surface albedo (α), and total cloud amount (N) are mean values over the measuring period. The terms 'melting' and 'dry' indicate whether surface temperatures were mainly at or below the freezing point, respectively.

Location	Surface type	Measuring period (days)	θ_a(2 m) (°C)	α(1·5 m)	N (1/10)
I	melting ice	53	4·7	0·55	4·6
II	melting snow	31	1·9	0·69	8·3
III	dry snow	41	−9·9	0·81	3·6
IV	dry ice	37	−8·5	0·56	3·7

the Aanderaa 2770 is 5 per cent (e.g. Bintanja *et al.*, 1991; Boot *et al.*, 1991; Bintanja *et al.*, 1993). These values apply to daily mean values only. The longwave radiative transfer model of location II is believed to give fairly accurate values (estimated precision 5 per cent) because of the frequent occurrence of low clouds (from which the downward emitted longwave radiation reaching the surface can be calculated with reasonable accuracy). The surface energy balance model used to compute the upward longwave fluxes at locations II, III, and IV is considered to yield accurate fluxes (estimated precision 2 per cent) because the results are calibrated by comparison with additionally measured quantities (Bintanja and Van den Broeke, 1994, 1995). Table I summarizes some characteristics of the four locations.

At each location, cloud coverage and cloud type (and at location II cloud-base height) were estimated by visual observation three to eight times per day. However, only total cloud coverage (henceforth also referred to as 'cloud amount') was used in the subsequent analysis. Furthermore, only daily mean fluxes will be used in the following.

TRANSMISSION OF SOLAR RADIATION THROUGH THE ATMOSPHERE

The transmission of solar radiation through a clear-sky atmosphere depends on the amount and vertical distribution of water vapour and ozone, Rayleigh scattering at air molecules and absorption and scattering at aerosols. Under overcast conditions, however, the transmission is determined mainly by the cloud properties (reflection and absorption), which are dependent on the cloud optical thickness ($\tau \approx 3$ LWC$/(2\rho_l r_e)$) (Stephens, 1984), where LWC is the liquid water content, ρ_l is the density of water, and r_e the effective cloud particle radius.

The form of the dependence of the incident shortwave radiative flux on total cloud amount can be determined from surface radiation measurements. The total effective transmission (T) is defined as the ratio of downward solar radiation at the surface and at the top of the atmosphere (note that according to this definition multiple reflection between surface and atmosphere acts to increase the effective transmission). The temporal variation in T during the period of measurement and its dependence on total cloud amount (N) is shown in Figure 2 for locations I and III. The clear-sky transmission at location III is about 0·8, whereas at location I, in relatively warm and moist conditions, it is approximately 0·7 (the presence of aerosols and differences in surface elevation may also slightly contribute to these differences). At location I the transmission occasionally drops below 0·2, whereas at location III it is always higher than 0·5. This can be attributed to differences in transmissivity under overcast conditions, and, therefore, to differences in shortwave cloud optical properties, as can be inferred from the lower panels of Figure 2.

In the following, we will neglect the influence of surface elevation on the atmospheric transmission. In agreement with Konzelmann *et al.* (1994), who analysed incident radiation data over West Greenland, we fitted the dependence of T on N with a second-order polynomial of the form:

$$T = T_{cl} + (T_{ov} - T_{cl})N^2 \tag{2}$$

in which T_{cl} and T_{ov} are the transmissivities under clear-sky and overcast conditions, respectively. This relationship indicates the weak dependence of T on N for small N, as can be seen from Figure 2. This weak dependence can be attributed to the fact that low cloud amount often inherently coincides with small optical thickness and vice versa (Atwater and Ball, 1981). The dependence of T on N becomes stronger for large N, and accordingly equation (2) is confirmed by data obtained at locations I and III. Several other observational studies have presented $T-N$

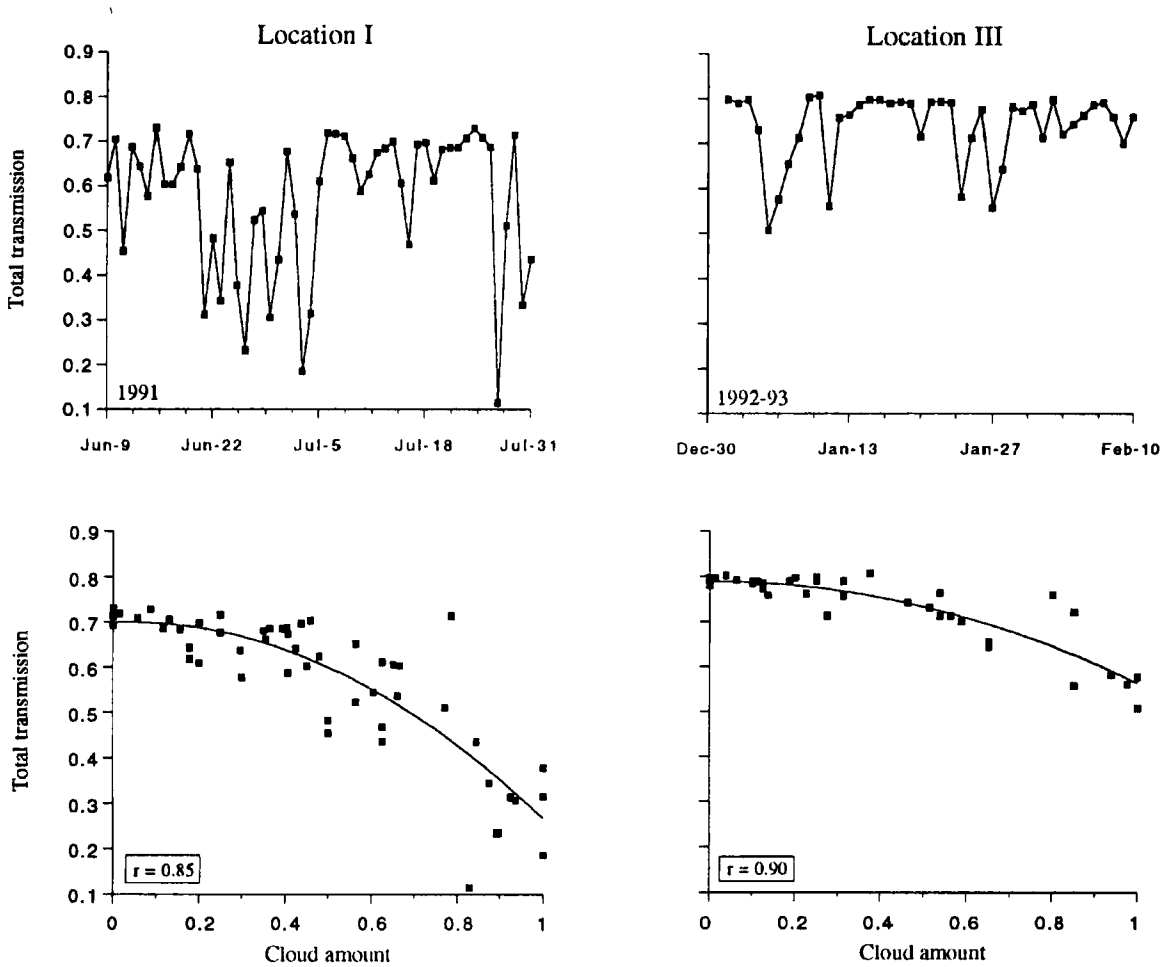

Figure 2. Variation in daily mean total transmission during the measuring period (upper panels) and dependence of daily mean total transmission on total cloud (lower panels) for locations I and III. In the lower panel, the line indicates the best fits of the form of equation (2). The correlation coefficient (r) is also given.

relationships that are qualitatively similar to the ones found here (e.g. Diamond and Gerdel, 1956; Ohmura, 1981; Dobson and Smith, 1989).

The mean values of the transmissivities, as derived from fitting equation (2) to the data, are presented in Table II for the various locations. Note that at location II, where daily mean cloud amount was always higher than 0·6, T_{cl} is unknown. However, because of the relatively warm and moist conditions at location II we expect T_{cl} to have a value of about 0·7. The main cause of the differences in T_{ov} between the various locations is the difference in shortwave cloud properties (optical thickness).

Another mechanism to explain high insolation values over highly reflective surfaces is multiple scattering between surface and cloud-base (e.g. Vowinckel and Orvig, 1962; Wiscombe, 1973; Schneider and Dickinson, 1976; Wendler *et al.*, 1981; Rouse, 1987). It has been shown that solar insolation over snow and ice are significantly enhanced (by as much as a factor of two) in comparison with low reflective surfaces (e.g. Wendler *et al.*, 1981). This effect will certainly influence the shortwave radiative fluxes under cloudy conditions in our case. Because the differences in surface albedo between the different locations is not so large, we expect that multiple reflection plays a minor role in explaining the differences in T_{ov} between the various locations.

One might expect that the value of the clear-sky transmissivity at location III equals that of location IV because of the small distance between these two locations. However, because the surrounding mountains obstruct the direct

Table II. Mean values of solar radiative flux at the top of the atmosphere ($S^{\downarrow}_{TOA}$) and at the surface ($S^{\downarrow}_{SFC}$), mean transmissivity (T) and mean transmissivity in clear-sky (T_{cl}) and overcast (T_{ov}) conditions at the four measuring locations. In order to calculate $S^{\downarrow}_{TOA}$ the solar constant was taken to equal 1360 W m^{-2} (Peixoto and Oort, 1992).

Location	$S^{\downarrow}_{TOA}$ (W m^{-2})	$S^{\downarrow}_{SFC}$ (W m^{-2})	T	T_{cl}	T_{ov}
I	459	262	0·57	0·70	0·28
II	502	225	0·45	–	0·35
III	448	330	0·74	0·78	0·57
IV	448	292	0·65	0·70	0·45

solar beam at large zenith angles at location IV, less solar radiation reaches the surface than at location III. Because of the increasing zenith angle during the measuring period, the duration of the shading increased, which led to lower values of T. Unfortunately, due to this mountain shading we are not able to quantify the influence of multiple scattering. The main feature in Table II and Figure 2 is the large variation in T_{ov} between the four locations; this variation is due most likely to differences in cloud properties (especially predominant cloud optical thickness).

THE SURFACE RADIATION BUDGET

Shortwave radiation

The net shortwave radiation budget over highly reflective surfaces is determined by a variety of processes, of which the following are the most important.

(i) Incident radiation at the surface, as described in the previous section. It is determined mainly by the amount and optical properties of clouds. As discussed in the previous section, a potentially important mechanism over highly reflective surfaces is the occurrence of multiple reflection between surface and cloud-base, which can lead to relatively large incident radiation values under overcast conditions (and hence high T_{ov}) (e.g. Wendler *et al.*, 1981; Rouse, 1987).

(ii) Surface albedo, which is dependent on surface characteristics (e.g. snow grain size). It also depends on other factors such as cloud amount, zenith angle, and precipitation/accumulation or ablation. The dependence of snow/ice albedo on cloud amount is twofold (Wiscombe and Warren, 1980): firstly, clouds convert direct radiation into diffuse radiation, thereby changing the effective zenith angle of the incoming radiation, and secondly, clouds absorb shortwave radiation at wavelengths where the spectral snow/ice albedo is small (Grenfell and Maykut, 1977). According to Carroll and Fitch (1981), the zenith angle effect is generally the main factor determining whether the snow albedo increases or decreases with increasing cloud amount. The effect of snow accumulation (often coinciding with large amount of cloud) is to increase the surface albedo. This is evident over ice, but this also occurs over snow surfaces (after deposition the snow particle size increases gradually, decreasing the albedo). In contrast, rain will lower the surface albedo, as will surface melt, because water (with relatively low albedo) starts to accumulate on the surface and the snow grain size increases dramatically.

The surface albedo over snow and ice will generally depend on cloud amount. However, the individual processes in this dependence are sometimes hard to unravel from measurements. Some indication is shown in Figure 3, in which the surface albedo (α) is plotted against cloud amount for locations II and IV. These are the two locations with the strongest dependence of α on N. At both locations, α seems to increase with increasing N; this is due mainly to the correlation between cloud amount and accumulation of fresh snow with high albedo. At location IV, the peaked values of α of up to 0·7 or more are connected to precipitation events. Because also drifting snow can cause new snow to accumulate (and hence change the grain size), the dependence of α on cloud amount due to the above-mentioned two 'radiation' reasons is obscured. At location II, with its relatively warm, maritime climate, surface melting during periods of low cloud amount further strengthens the α–N relationship.

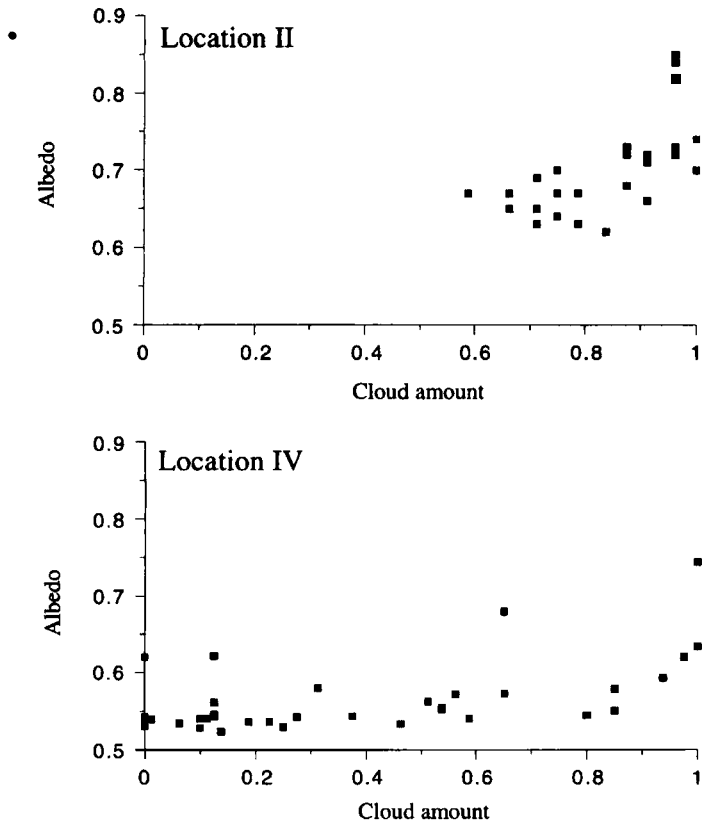

Figure 3. Daily mean surface albedo as a function of total cloud amount for locations II and IV.

Table III. Slopes of the linear fits of the dependence of net shortwave radiation ($\delta S/\delta N$), net longwave radiation ($\delta L/\delta N$) and net radiation ($\delta R/\delta N$) on total cloud amount at the four measuring locations (in W m^{-2}). The linear fits are shown in Figures 4–6.

Location	$\delta S/\delta N$	$\delta L/\delta N$	$\delta R/\delta N$
I	−82	+61	−21
II	−152	+65	−87
III	−31	+56	+25
IV	−56	+85	+29

The dependence of the net shortwave radiation (S) on cloud amount is shown in Figure 4 for each location. Also shown are the best linear fits to the data (coefficients tabulated in Table III), although it is realized that the dependence of S on N may be strongly non-linear (e.g. see equation (2)). These best linear fits merely yield an order-of-magnitude estimate of the slopes. The fact that the largest decrease of S with N occurs at locations I and II can be attributed mainly to the small cloud transmissivity under cloudy conditions at these sites (see Table II).

Longwave radiation

Under cloud-free conditions, the incoming longwave radiation at the surface ($L\downarrow$) is determined mainly by the temperature and humidity distribution in the lowest atmospheric layers (approximately 90 per cent of $L\downarrow$ at the surface originates from the lowest 1 km (W. Greuell, pers. comm., 1995). In overcast conditions, $L\downarrow$ is almost

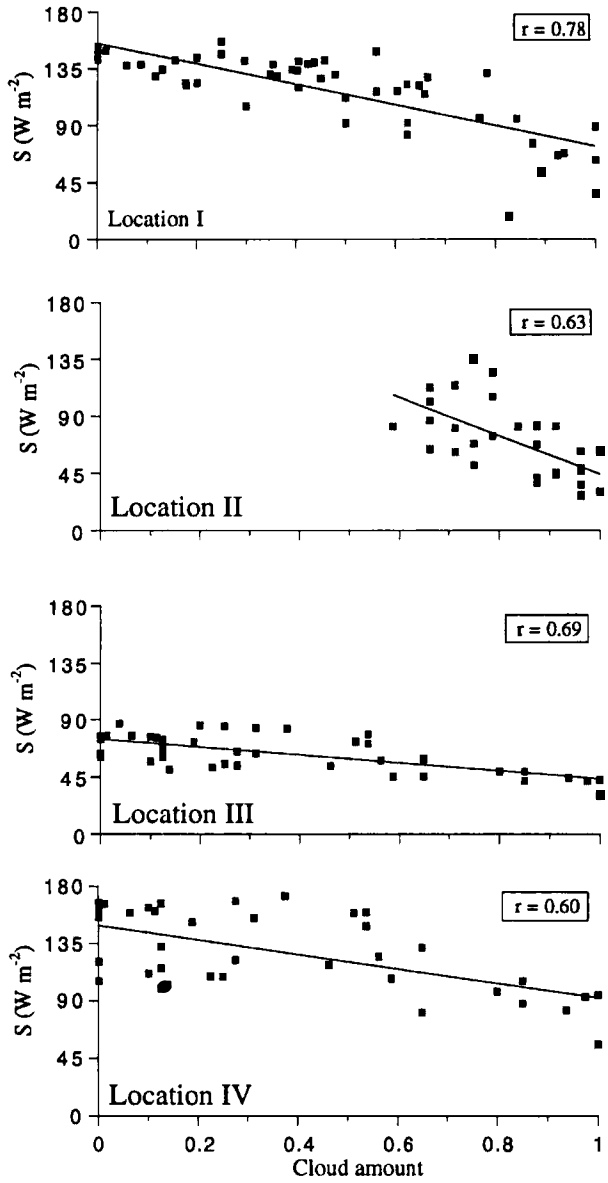

Figure 4. Dependence of daily mean net shortwave radiation (S) on total cloud amount at the four locations. The lines indicate the best linear fits to the data whose slopes are given in Table III. The correlation coefficient (r) is also given.

completely determined by the temperature (and hence height) of the cloud base. Nearly all clouds can be considered black for infrared radiation, which means that their emissivity is equal to 1, except for optically thinnest clouds (e.g. cirrus, arctic stratus (Tsay *et al.*, 1989)).

Generally, snow/ice surfaces are assumed to be virtually black for infrared radiation (Brutsaert, 1982). The surface emits longwave radiation ($L\uparrow$) at the surface radiation temperature. This causes the average upward longwave radiation to be approximately equal to 315 W m^{-2} at locations where the surface is (nearly) continuously at melting point (at locations I and II). However, when the surface temperature is well below 0°C and temporal variations in $L\uparrow$ are possible (at locations III and IV), the temporal variations in $L\uparrow$ nevertheless seem to be smaller than those in $L\downarrow$. This is due to the thermal capacity of the upper few metres of the snow/ice, which prevents the daily mean surface temperature from changing rapidly during summer. In contrast, variations in cloud-

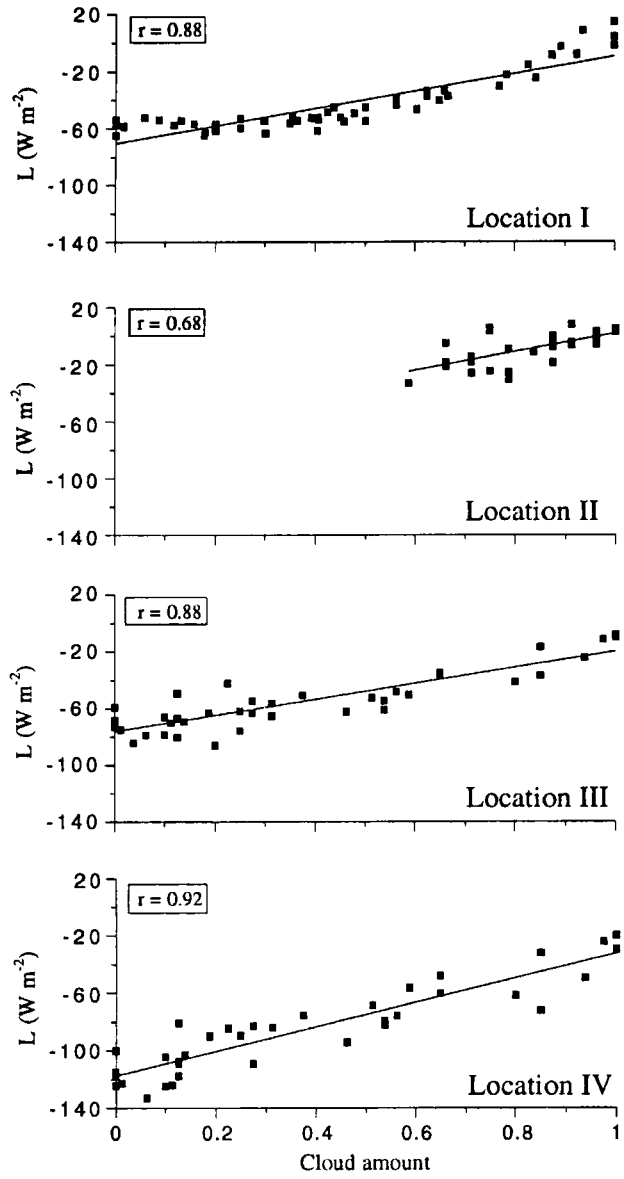

Figure 5. As in Figure 4 but for daily mean net longwave radiation (L). Note that for location I the incoming longwave radiation is estimated using equation (1).

base temperature, cloud amount, and cloud emissivity are not subject to such restrictions, which causes larger variations in daily mean values of $L\downarrow$. Therefore, the dependence of net longwave radiation on cloud amount is due mainly to variations in $L\downarrow$.

The dependence of net longwave radiation (L) on cloud amount at each location is shown in Figure 5. Considering the linear regression coefficients in Table III, the increase in L with N does not vary much between the four locations (by less than 30 W m^{-2}, which is obviously much smaller than the spatial variations in $\delta S/\delta N$). The increase of L with N measured by Yamanouchi and Kawaguchi (1984) at Mizuho Station, Antarctica, during austral summer (62 W m^{-2}) is in good agreement with the values presented here. Furthermore, they observed that the increase of $L\downarrow$ with N from clear to overcast is about 77 W m^{-2} and the increase of $L\uparrow$ with N is about 15 W m^{-2} (in summer), which agrees with our finding that the variation of $L\uparrow$ with N is due mainly to variations in $L\downarrow$.

The phenomenon that $\delta L/\delta N$ is spatially more homogeneous than $\delta S/\delta N$ is due largely to the fact that cloud shortwave properties are dependent on LWC over a larger range of LWC compared with the cloud longwave emissivity; above a certain value of LWC the emissivity equals unity, whereas the cloud albedo can further increase with increasing LWC (Stephens and Webster, 1981). The consequence of the emissivity of clouds being unity for almost every cloud type is that the dependence of L on N has a strong linear component, as confirmed experimentally by Ohmura (1981).

An interesting feature is the relatively large difference in $\delta L/\delta N$ between location III and the nearby situated location IV. Because incoming longwave radiation at these two sites is almost identical, this difference must be caused by large spatial variations in $L\uparrow$. At location IV strong solar heating takes place over the blue ice during clear-sky conditions (see Figure 4). As a result, the blue ice at location IV us substantially warmer than the snow surface at location III during cloud-free conditions. Consequently, over blue ice (location IV), $\delta L\uparrow/\delta N$ is larger than over snow (location III).

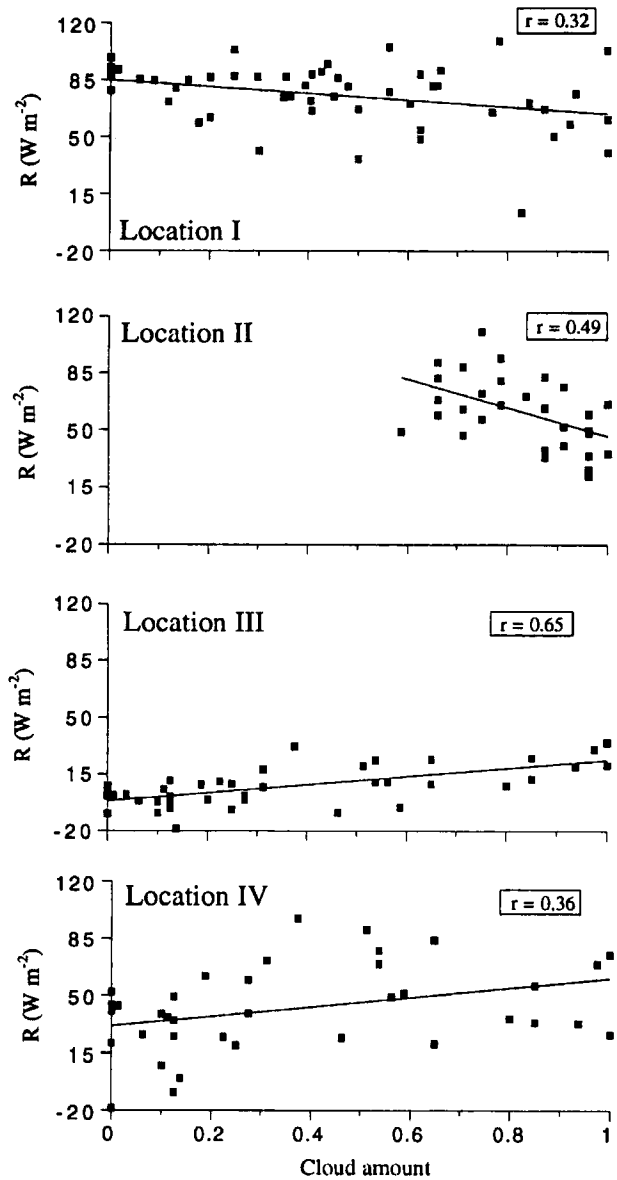

Figure 6. As in Figure 4 but for daily mean net radiation (R).

Net radiation

The variation of net radiation with cloud amount is depicted in Figure 6. The best linear fits to the data indicate that only at locations III and IV does the net radiation increase with cloud amount (see Table III). Small values of T_{ov} (and hence large values of $\delta S/\delta N$) cause a decrease in net radiation with increasing cloud amount at locations I and II. In accordance with some previously published results we find that the net radiation increases with cloud amount over snow with high albedo (location III) (e.g. Holmgren, 1971, Jacobs *et al.*, 1972; Ambach, 1974; Ohmura, 1981; Yamanouchi *et al.*, 1982; Wendler, 1986). Surprisingly, this also occurred over blue ice (location IV) with its relatively low albedo; this is caused mainly by the low opacity of the predominant clouds. It therefore can be concluded that, during summer, the occurrence of an increasing net radiation with increasing cloud amount at a specific location depends not only on the value of the surface albedo, but also on the rate at which incoming shortwave radiation decreases with cloud amount, and hence on the effective cloud transmissivity under conditions with large amounts of cloud. Therefore, it seems appropriate to analyse the dependence of the net radiation on cloud amount in terms of surface albedo and effective cloud transmissivity.

THE DEPENDENCE OF THE RELATION BETWEEN NET RADIATION AND CLOUD AMOUNT ON SURFACE ALBEDO AND CLOUD TRANSMISSIVITY

From summertime radiation data over four types of highly reflective surfaces it was found that the surface albedo and the effective cloud transmissivity are important variables in the dependence of the net surface radiation budget on total cloud amount. To investigate under what circumstances the net radiation increases with increasing cloud amount at a certain location, we assumed the net radiation to be a function of three variables, i.e. N, α, and T (and also of the solar flux at TOA (top of the atmosphere)). Further, we assume that $\delta L/\delta N$ is independent of N, in agreement with radiation measurements presented by Ohmura (1981). Although this is certainly not evident from the data and even contradicts with equation (1), the form of $\delta L/\delta N$ is much less important than that of $\delta S/\delta N$ because spatial variations in $\delta S/\delta N$ are much larger than those in $\delta L/\delta N$ (see Table III). Further, α is assumed to be independent of N. Although this is not valid at all locations considered here (see Figure 3), the form of the dependence of α on N differs significantly between the four locations, which makes it impossible to use a general α–N relationship. With the use of equation (2), the daily mean net radiation budget (R) can simply be expressed in terms of α and N:

$$R = S^{\downarrow}_{TOA}(1-\alpha)\{T_{cl} + (T_{ov} - T_{cl})N^2\} + L_0 + N\frac{\partial L}{\partial N} \tag{3}$$

where $S^{\downarrow}_{TOA}$ is the daily mean shortwave incoming radiation at the top of the atmosphere, L_0 is the net longwave radiation in the absence of clouds, and $\delta L/\delta N$ is the slope of the linear dependence of the net longwave radiation on N. Using this simple expression, which is based essentially on data obtained at the four locations, the dependence of R on N can be crudely investigated. Note that at the four locations studied, the mean value of $S^{\downarrow}_{TOA}$ over the respective measuring period is 450 to 500 W m^{-2} (Table II). We will further use a value of 500 W m^{-2} for $S^{\downarrow}_{TOA}$, a value that is typical for midsummer daily averaged insolation at the top of the atmosphere in the polar regions. Furthermore, variations in T_{ov} between the three locations (I, III and IV) are much larger than variations in T_{cl} (see Table III and Figure 2). The value of T_{cl} ($=0{\cdot}75$) is therefore taken to be constant.

If the surface albedo is assumed to be constant, the sign of $\delta R/\delta N$ depends mainly on the value of T_{ov} as can be inferred from Figure 7. Obviously, it is much more likely to have $\delta R/\delta N > 0$ if T_{ov} is relatively large, that is, if the cloud optical depth is small. For optically thicker clouds, $\delta R/\delta N$ becomes negative for large N, whereas for small N the net radiation increases with increasing cloud amount. This can be understood from Figure 2, because at small N the variation of net solar radiation with cloud amount is negligible. Thus, for thin clouds, which are usually present for small N, the increase in $L\downarrow$ with N is larger than the decrease in S. An increase in net radiation with increasing cloud amount is less likely to be observed for small T_{ov}.

These results qualitatively agree with the model calculations of Stephens and Webster (1981), from which it can be inferred that the optically thinnest clouds have the strongest warming effect (remember that, generally, cloud amount and cloud optical thickness are correlated (Atwater and Ball, 1981)). Stephens and Webster (1981) attribute this to the fact that, for thin clouds, the numerical value of cloud emissivity is much larger than that of cloud

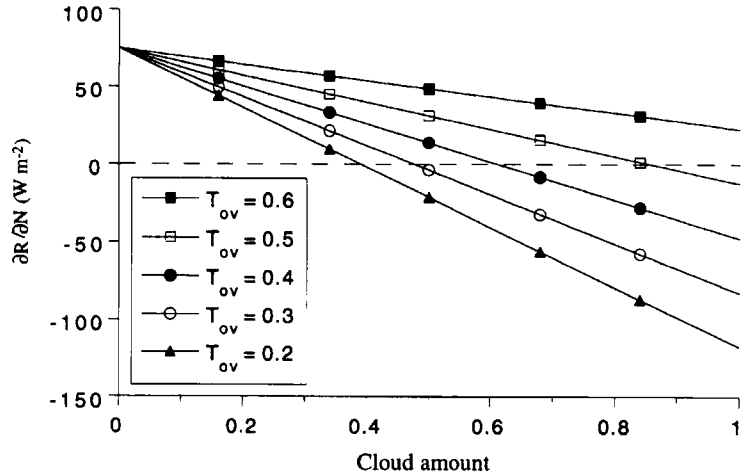

Figure 7. Dependence of $\delta R/\delta N$ on cloud amount for various values of the transmissivity under overcast conditions (T_{ov}), as calculated with equation (3). The following values have been used: $\alpha = 0{\cdot}65$, $T_{cl} = 0{\cdot}75$ and $\delta L/\delta N = 75$ W m^{-2}.

albedo, so that longwave warming outweighs shortwave cooling. Increasing the cloud optical depth causes a large increase in cloud albedo and only a small change in cloud emissivity so that the cooling effect starts to dominate. This explains why $\delta R/\delta N$ is less likely to be positive for large cloud amount, as also observed by Ohmura (1981).

The simultaneous dependence of $\delta R/\delta N$ on α and T_{ov} is depicted in Figure 8(a). As expected, an increase in R with increasing N is likely to occur when both α and T_{ov} are large (e.g. at location III) and less likely when both α and T_{ov} are small (e.g. at location I). Figure 8(b) shows lines of $\delta R/\delta N = 0$ for various values of T_{ov} as a function of α and N. The figure shows for which value of T_{ov} one can expect positive values of $\delta R/\delta N$ when α and N are known. If T_{ov} is large enough, $\delta R/\delta N > 0$ even if α is small (e.g. location IV). In case of thicker clouds (hence smaller T_{ov}), R can increase with increasing N only if α is large enough. It must be noted that the results displayed in Figures 7 and 8 will not change significantly if a realistic non-linear relationship between L and N (e.g. equation (1)) is used instead of a linear one.

Our results suggest that T_{ov} and α are of practically equal importance with regard to the slope of the R–N relation, especially at high cloud amount. This is due to the fact that clouds with similar large values of optical thickness can have significantly different shortwave optical properties but will have similar values of longwave emissivity (Stephens and Webster, 1981). Thus, the phenomenon that net radiation increases with increasing cloud amount is, under favourable conditions (e.g. high albedo), attributable to the asymmetry in the dependency of the longwave and shortwave radiative cloud properties on cloud optical thickness.

Ambach (1977) used radiation data obtained over the Greenland ice sheet to relate the occurrence of $\delta R/\delta N > 0$ to surface albedo and incident solar radiation. He found that an increase in net radiation with increasing cloud amount occurred only in the accumulation zone with high albedo and not in the ablation zone; this result is in accordance with the results presented here. He also noticed that the sign of $\delta R/\delta N$ depended on the amount of incident radiation at the top of the atmosphere, in accordance with the modelling results of Stephens and Webster (1981). Because the shortwave incident radiation at the surface is directly proportional to the downward solar flux at the top of the atmosphere (see equation (3)), this seems to be a straightforward statement.

Obviously, an increase in net radiation with increasing cloud amount occurs throughout the winter when incident shortwave radiative fluxes are small or absent (e.g. Curry and Ebert, 1992; Schweiger and Key, 1994). In summer, the sign of $\delta R/\delta N$ will become negative only when the net surface solar radiation reaches a certain level. Schweiger and Key (1994) calculated the annual cycle of the radiative fluxes in the Arctic basin and found that $\delta R/\delta N < 0$ during 4 months in summer, when albedo values dropped to about 0·4. They also found that minimum values of $\delta R/\delta N$ tend to increase going northward, which can be attributed mainly to the fact that the surface albedo increases in the northward direction. In another modelling study about the effects of clouds on radiation over the Arctic Ocean, Curry and Ebert (1992) found that net radiation increased with increasing cloud amount throughout the year, except for 2 weeks in summer when surface albedos dropped to 0·5. Detailed radiative

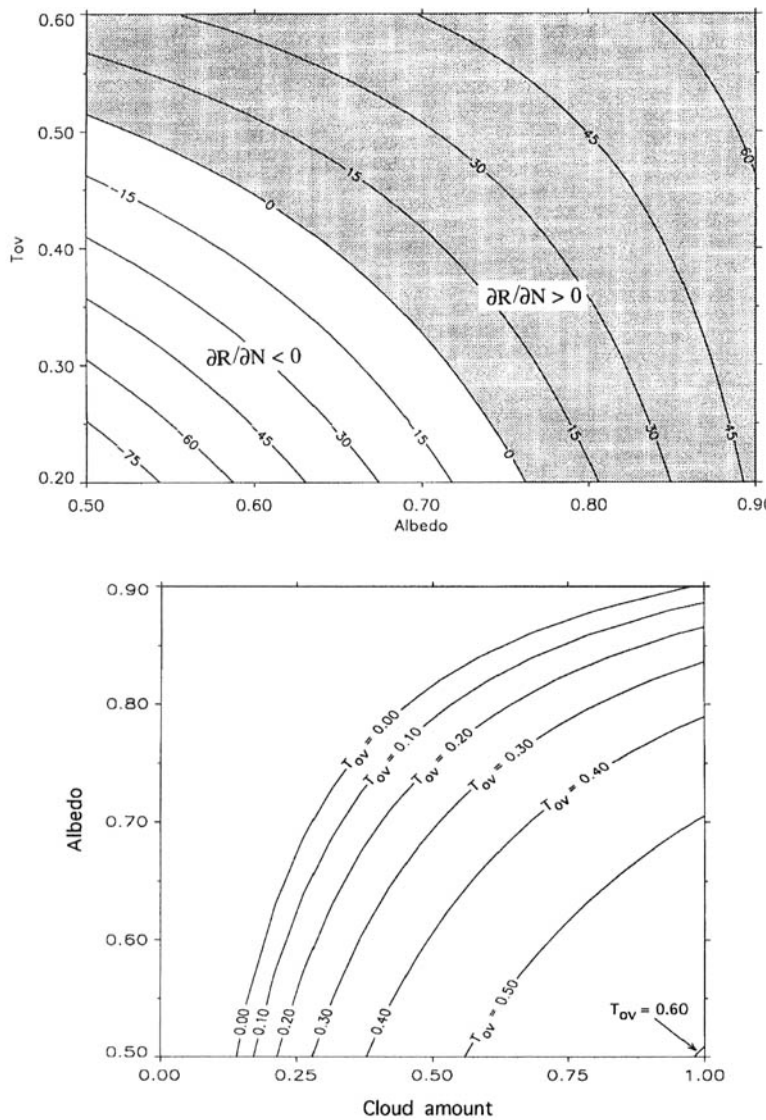

Figure 8(a) Dependence of $\delta R/\delta N$ (W m^{-2}) on the transmissivity under overcast conditions (T_{ov}) and albedo according to equation (3). The following values have been used: $N = 0{\cdot}5$, $T_{cl} = 0{\cdot}75$ and $\delta L/\delta N = 75$ W m^{-2}. (b) Lines of $\delta R/\delta N = 0$ W m^{-2} as a function of albedo and cloud amount for various values of the transmissivity under overcast conditions (T_{ov}). The value of $\delta R/\delta N$ increases towards the upper-left corner. For instance, $\delta R/\delta N > 0$ W m^{-2} for almost each value of α and N for $T_{ov} = 0{\cdot}6$. The following values have been used: $T_{cl} = 0{\cdot}75$ and $\delta L/\delta N = 75$ W m^{-2}.

calculations made by Tsay *et al.* (1989) indicate that arctic stratus clouds have a net radiative cooling effect at the surface in June (with an albedo of 0·57). Our analysis indicates that $\delta R/\delta N > 0$ can persist throughout the year over regions with high surface albedo and/ or with a predominantly optically thin cloud cover, and that net radiation can decrease with increasing cloud amount otherwise (in summer).

DISCUSSION AND CONCLUSIONS

Another way to quantify the influence of clouds on the radiation budget of the surface is to use the term cloud radiative forcing (CRF). The shortwave (CRF_s) and longwave (CRF_L) cloud radiative forcing at the surface are defined as:

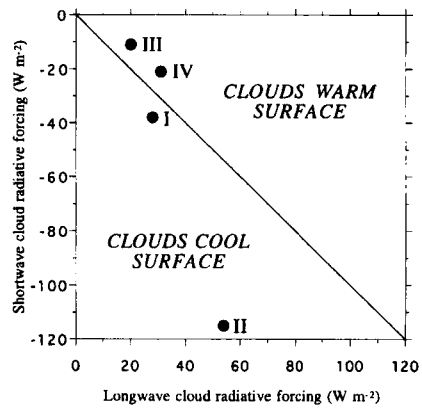

Figure 9. Period mean values of cloud surface radiative forcing for each location. Clouds cool the surface at locations I and II, whereas they warm the surface at locations III and IV. Note that because S_{cl} could not be measured at location II, its value was estimated assuming $T_{cl} = 0{\cdot}75$ and $\alpha = 0{\cdot}69$.

$$\begin{aligned} \mathrm{CRF_S} &= N[\mathrm{S_{ov}} - \mathrm{S_{cl}}] \\ \mathrm{CRF_L} &= N[\mathrm{L_{ov}} - \mathrm{L_{cl}}] \end{aligned} \tag{4}$$

where the subscripts $_{\mathrm{cl}}$ and $_{\mathrm{ov}}$ represent clear-sky and overcast conditions, respectively. The term cloud radiative forcing was introduced some years ago to quantify the influence of clouds on the radiation at the top of the atmosphere (e.g. Hartmann *et al.*, 1986). Because $\mathrm{CRF_L}$ is normally positive, clouds warm the surface in the longwave region, whereas clouds cool the surface in the shortwave region ($\mathrm{CRF_S} < 0$). From Figure 9, where the four locations are plotted according to their respective CRF, it can be readily inferred that clouds warm the surface at locations III and IV, whereas they cool the surface at locations I and II. This can be interpreted as a decrease (increase) in net radiation with increasing cloud amount at locations I and II (III and IV).

At location I, the radiative cooling due to clouds is less strong than that over the Arctic Ocean, where July net cloud forcing amounts to -47 W m^{-2} (Schweiger and Key, 1994). Because the $\mathrm{CRF_L}$ values are comparable, the differences in net cloud forcing arise from differences in $\mathrm{CRF_S}$. Apart from possible differences in cloud properties (clouds near the tundra in west Greenland may be optically thicker than arctic stratus), this is due to differences in surface albedo (0·55 at location I versus 0·4 over the Arctic Basin).

As part of the ongoing discussion about predictions of cloud amount using climate models, this study gives insight into the relation between possible future changes in cloud amount and changes in the surface radiative fluxes over snow and ice surfaces. Because radiation provides a considerable portion of the energy for melting in the ablation zones of glaciers and ice sheets (Greuell and Konzelmann, 1994; Bintanja, 1995), this study may eventually lead to a better understanding of the impact of variations in cloud amount on the surface mass balance.

On large ice sheets such as Antarctica and especially Greenland, the increase in surface albedo from the ice-edge toward the interior generally coincides with a decrease in cloud amount (Vowinckel and Orvig, 1970; Schweiger and Key, 1992) and cloud optical thickness. The thinning of clouds going up the ice sheet can be attributed mainly to enhanced subsidence toward the interior. Both factors lead to an increase of $\delta R/\delta N$ from the low ablation zone toward the higher accumulation zone (see also Figure 8(a). As a result, in the presence of clouds the surface mass balance gradient with height will be weaker than in cloud-free conditions (note that surface ablation due to an excess of net radiative energy significantly affects the surface mass balance gradient along an ice sheet). In this light, one may speculate that after a uniform increase (decrease) in cloud amount as a part of climate change the surface mass balance gradient with height of the major ice sheets will become smaller (larger); this, in turn, might have important implications for variations in the integrated mass balance of these ice sheets (and hence for sea-level changes).

The main conclusion of the present study is that whether or not net surface radiation increases with increasing cloud amount over highly reflective surfaces during summer depends dominantly on two factors: (i) the surface albedo and (ii) the predominant cloud transmissivity. We have been able to investigate the dependence of the net radiation on cloud amount in terms of surface albedo and cloud optical properties using summertime radiation data over four different types of highly reflective surfaces.

ACKNOWLEDGEMENTS

We are grateful to the many people who were in some way involved in the three field campaigns. Wouter Greuell, Roderik van de Wal, and Hans Oerlemans are thanked for their useful suggestions on earlier versions of the manuscript. Financial support was provided by the Netherlands Antarctic Research Programme (GOA) and the Dutch National Research Programme on Global Air Pollution and Climate Change (NOP).

REFERENCES

Ambach, W. 1977. 'Untersuchungen zum Energieumsatz in der Ablationzone des grönlandischen Inlandeises. Nachtag', *Medd. Grønl.*, **187**, (5).

Ambach, W. 1984. 'The influence of cloudiness on the net radiation balance of a snow surface with high albedo', *J. Glaciol.*, **13** (67), 73–84.

Arking, A. 1991. 'The radiative effects of clouds and their impact on climate', *Bull. Am. Meteorol. Soc.*, **72**, 795–813.

Atwater, M. A. and Ball, J. T. 1980. 'A surface solar radiation model for cloudy atmospheres', *Mon. Wea. Rev.*, **109**, 878–888.

Bintanja, R. 1992. 'Glaciological and meteorological investigations on Ecology Glacier, King George Island, Antarctica (summer 1990–1991)', *Circumpolar J.*, **7**, 59–71.

Bintanja, R. 1995. 'The local surface energy balance of the Ecology Glacier, King George Island, Antarctica: measurements and modelling', *Antarctic Sci.*, **7**, 315–325.

Bintanja, R. and Van den Broeke, M. R. 1994. 'Local climate, circulation and surface energy balance of an Antarctic blue ice area', *Ann. Glaciol.*, **20**, 160–168.

Bintanja, R. and Van den Broeke, M. R. 1995. 'The surface energy balance of Antarctic snow and blue ice', *J. Appl. Meteorol.*, **34**, 902–926.

Bintanja, R., Conrads, L. A., Oerlemans, J. and Portanger, M. J. 1991. *Glacio-meteorological investigations on Ecology Glacier, summer 90–91, King George Island, Antarctica*, Arctowski-90/91 Field Report, Internal Report of the Institute for Marine and Atmospheric Research Utrecht, Utrecht University, 17 pp.

Bintanja, R., Van den Broeke, M. R. and Portanger, M. J. 1993. *A Meteorological and Glaciological Experiment on a Blue Ice Area in the Heimefront Range, Queen Maud Land, Antarctica*, SVEA Field Report, Internal Report of the Institute for Marine and Atmospheric Research Utrecht, Utrecht University, 29 pp.

Boot, W., Van den Broeke, M. R., Conrads, L. A., Duynkerke, P. G., Oerlemans, J., Portanger, M. J., Russell, A. J., Snellen, H. and Van de Wal, R. S. W. 1991. *GIMEX-91 Field Report*, Internal Report of the Institute for Marine and Atmospheric Research Utrecht, Utrecht University, 18 pp.

Brutsaert, W. H. 1982. *Evaporation into the Atmosphere*, Reidel, Dordrecht, 299 pp.

Carroll, J. J. and Fitch, B. W. 1981. 'Effects of solar elevation and cloudiness on snow albedo at the South Pole', *J. Geophys. Res.*, **86**, 5271–5276.

Crane, R. G. and Barry, R. G. 1984. 'The influence of clouds on climate with a focus on high latitude interactions', *J. Climatol.*, **4**, 71–93.

Curry, J. A. and Ebert, E. E. 1992. 'Annual cycle of radiation fluxes over the Arctic Ocean: sensitivity to cloud optical properties', *J. Climate.*, **5**, 1267–1280.

Diamond, M. and Gerdel, R. W. 1956. *Radiation Measurements on the Greenland Ice Cap*, U.S. Army, Corps Engineers, Snow, Ice, Permafrost Research Establishment, Research Report, 25.

Dobson, F. W. and Smith, S. D. 1989. 'A comparison of incoming solar radiation at marine and continental stations', *Q. J. R. Meterorol. Soc.*, **115**, 353–364.

Grenfell, T. C. and Maykut, G. A. 1977. 'The optical properties of ice and snow in the Arctic basin', *J. Glaciol.*, **18**, 445–463.

Greuell, W. and Konzelmann, T. 1994. 'Numerical modelling of the energy balance and the englacial temperature of the Greenland Ice Sheet. Calculations of the ETH-Camp location (West Greenland, 1155 m a.s.l.)', *Global Planet. Change*, **9**, 91–114.

Hartmann, D. L., Ramanathan, V., Berroir, A. and Hunt, G. E. 1986. 'Earth radiation budget data and climate research', *Rev. Geophys.*, **24**, 439–468.

Holmgren, B. 1971. 'Climate and energy budget on a sub-polar ice cap in summer. Part F: On the energy exchange of the snow surface at Ice Cap Station', *Meteorol. Inst. Uppsala univ. Medd.*, **112**, 53 pp.

Jacobs, J. D., Andrews, J. T., Barry, R. G., Bradley, R. S., Weaver, R. and Williams, L. D. 1972. 'Glaciological and meteorological studies on the Boas Glacier, Baffin Island, for two contrasting seasons (1969-70 and 1970-71)', in *The Role of Snow and Ice in Hydrology*, IAHS-AISH Publication No. 107, Vol. 1.

Konzelmann, T., Van de Wal, R. S. W., Greuell, W., Bintanja, R., Henneken, E. A. C. and Abe-Ouchi, A. 1994. 'Parameterization of global and longwave incoming radiation for the Greenland Ice Sheet', *Global Planet. Change*, **9**, 143–164.

Li, Z. and Leighton, H. G. 1991. 'Scene identification and its effect on cloud radiative forcing in the Arctic', *J. Geophy S. Res.*, **96**, 9175–9188.

Manabe, S. and Wetherland, R. J. 1967. 'Thermal equilibrium of the atmosphere with convective adjustment', *J. Atmos. Sci.*, **24**, 241–259.

McClatchey, R. A., Fenn, R. W., Selby, J. E., Volts, F. E. and Garing, J. S. 1971. *Optical Properties of the Atmosphere*, 3rd ed., AFCRL-72-0497.

Nakamura, N. and Oort, A. H. 1988. 'Atmospheric heat budgets of the polar regions', *J. Geophys. Res.*, **93**, 9510–9524.

Nemesure, S., Cess, R. D., Dutton, E. G., DeLuisi, J. J., Li, Z. and Leighton, H. G. 1994. 'Impact of clouds on the shortwave radiation budget of the surface–atmosphere system for snow-covered surfaces', *J. Climate*, **7**, 579–585.

Oerlemans, J. and Vugts, H. F. 1993. 'A meteorological experiment in the melting zone of the Greenland ice sheet', *Bull. Am. Meteorol. Soc.*, **74**, 35–365.

Ohmura, A. 1981. 'Climate and energy balance of Arctic tundra', *Z. Geogr. Schrift.*, **3**, 448 pp.

Peixoto, J. P. and Oort, A. H. 1992. *Physics of Climate*, American Institute of Physics, New York, 520 pp.

Rouse, W. R. 1987. 'Examples of enhanced global solar radiation through multiple reflection from an ice-covered Arctic sea', *J. Clim. Appl. Meteorol.*, **26**, 670–674.

Schneider, S. 1972. 'Cloudiness as a global feedback mechanism: the effects on the radiation balance and surface temperature of variation in cloudiness', *J. Atmos. Sci.*, **29**, 1413–1422.

Schneider, S. and Dickinson, R. E. 1976. 'Parameterization of fractional cloud amounts in climate models: the importance of modeling multiple reflections', *J. Appl. Meteorol.*, **15**, 1050–1056.

Schweiger, A. J. and Key, J. R. 1992. 'Arctic cloudiness: comparison of ISCCP-C2 and Nimbus-7 satellite-derived cloud products with a surface-based cloud climatology', *J. Climate*, **5**, 1514–1527.

Schweiger, A. J. and Key, J. R. 1994. 'Arctic Ocean radiative fluxes and cloud forcing estimated from the ISCCP C2 cloud dataset, 1983–1990', *J. Appl. Meteorol.*, **33**, 948–963.

Stephens, G. L. 1984. 'The parameterization of radiation for numerical weather prediction and climate models', *Mon. Wea. Rev.*, **112**; 826–867.

Stephens, G. L. and Webster, P. J. 1981. 'Clouds and climate: sensitivity of simple systems;, *J. Atmos. Sci.*, **38**, 235–247.

Stephens, G. L., Campbell, G. G. and Vonder Haar, T. H. 1981. 'Earth radiation budgets', *J. Geophys. Res.*, **86**, 9739–9760.

Tsay, S. C., Stamnes, K. and Jayaweera, K. 1989. 'Radiative energy budget in the cloudy and hazy Arctic', *J. Atmos.Sci.*, **46**, 1002–1018.

Vowinckel, E. and Orvig, S. 1962. 'Relation between solar radiation income and cloud type in the Arctic', *J. Appl. Meteorol.*, **1**, 552–559.

Vowinckel, E. and Orvig, S. 1970. 'The climate of the North Polar Basin', in Orvig, S. (ed.), *World Survey of Climatology*, Vol. 14, 129–252.

Wendler, G. 1986. 'The "Radiation Paradox" on the slopes of the Antarctic continent', *Polarforschung*, **56 (1/2)**, 33–41.

Wendler, G., Eaton, F. D. and Ohtake, T. 1981. 'Multiple reflection effects on irradiance in the presence of Arctic Stratus clouds', *J. Geophys. Res.*, **86**, 2049–2057.

Wiscombe, W. J. 1983. 'Solar radiation calculations for Arctic summer stratus conditions', in G. Weller and S. A. Bowling (eds), *Climate of the Arctic*, 24th Alaska Scientific Conference, Geophysical Institute, University of Alaska, 245–254.

Wiscombe, W. J. and Warren, S. G. 1980. 'A model for the spectral albedo of snow. I: pure snow', *J. Atmos. Sci.*, **37**, 2712–2733.

Yamanouchi, T. and Kawaguchi,S. 1984. 'Longwave radiation balance under a strong surface inversion in the katabatic wind zone, Antarctica', *J. Geophys. Res.*, **89**, 11771–11778.

Yamanouchi, T., Wada, M., Mae, S., Kawaguchi, S. and Kusunoki, K. 1982. 'The radiation budget at Mizuho Station', *Ann. Glaciol.*, **3**, 327–332.